



DEVELOPMENT OF THE TURBULENT SWIRLING FLOW VELOCITY PROFILES IN THE AXIAL FAN JET

Novica Z. JANKOVIĆ¹, Đorđe S. ČANTRAK², Dejan B. ILIĆ³,
Miloš S. NEDELJKOVIĆ⁴

¹Corresponding Author. Department of Hydraulic Machinery and Energy Systems, University of Belgrade - Faculty of Mechanical Engineering, Kraljice Marije 16, 11120 Belgrade, Serbia. Tel.: +38 1 11 3302 363, E-mail: njankovic@mas.bg.ac.rs

²Corresponding Author. Department of Hydraulic Machinery and Energy Systems, University of Belgrade - Faculty of Mechanical Engineering, Kraljice Marije 16, 11120 Belgrade, Serbia. Tel.: +38 1 11 3302 226, E-mail: djcantrak@mas.bg.ac.rs

³Corresponding Author. Department of Hydraulic Machinery and Energy Systems, University of Belgrade - Faculty of Mechanical Engineering, Kraljice Marije 16, 11120 Belgrade, Serbia. Tel.: +38 1 11 3302 226, E-mail: dilic@mas.bg.ac.rs

⁴Department of Hydraulic Machinery and Energy Systems, University of Belgrade - Faculty of Mechanical Engineering, Kraljice Marije 16, 11120 Belgrade, Serbia. Tel.: +38 1 11 3302 226, E-mail: mnedeljkovic@mas.bg.ac.rs

ABSTRACT

Turbulent swirling flow in the jet generated by the axial fan impeller with twisted blades is studied in this paper. Three velocity components are obtained by using three-component laser Doppler velocimetry system in ten measured sections. Downstream flow development and continual deformation of all velocity profiles with gradients in radial and axial directions are obvious. It is shown that circumferential velocity significantly deforms profile of the axial velocity which gets M-shape with weak reverse flow region in the central flow zone in the first two measuring sections. This phenomenon is still not well explained, especially from the mathematical point of view.

Derivatives of all three velocity components in radial direction are calculated for velocity field analysis. Axial velocity profile in the downstream sections becomes more uniform, with the strict hierarchy of the positive gradient of the axial velocity in axial direction in domain $0 < r/R < 0.5$. Character of distribution of the axial velocity out of this region shows jet expansion. Maximum of the axial velocity doesn't belong to the jet core. In the jet axis vicinity profile of the axial velocity is concave even in the last measuring section. It means that the transformation process is not completed.

Keywords: axial fan, jet, swirling flow, three-component LDV, turbulence

NOMENCLATURE

C	[m/s]	total velocity
D	[m]	inner pipe diameter
Q	[m ³ /s]	volumetric flow rate
R	[m]	inner pipe radius
U	[m/s]	mean axial velocity

U_m	[m/s]	averaged velocity by area
V	[m/s]	mean radial velocity
W	[m/s]	mean circumferential velocity
r	[m]	radial coordinate
n	[rpm]	fan shaft rotation speed
x	[m]	axial coordinate along a jet axis
Γ	[m ² /s]	average circulation
Ω	[-]	swirl flow parameter
ν	[m ² /s]	kinematic viscosity
φ	[°]	coordinate of the polar cylindrical coordinate system (x, r, φ)

1. INTRODUCTION

In this paper is presented experimental research of the turbulent swirling flow in jet generated with the axial fan impeller with twisted blades. Axial fan is in-built in the installation following the setup category A for fans in the international standard ISO 5801 [1]. This installation means free inlet and free outlet.

Experimental research is performed by use of the three-component laser Doppler velocimetry (LDV) system.

A significant number of papers analyze free swirling jets, but only few of them investigate swirling jets generated by the axial fan impeller. A good literature overview of the turbulent swirling flow jet experimental research is presented in [2, 3]. In paper [4] is shown that the entrainment rate and angle of spread for the swirling jet was nearly twice that of the non-swirling free jet.

Study of jets with different initial swirl distributions is presented in [5]. In this case miniature five-hole probe is used for three-

component velocity measurements. Experimental study on the effects of swirl on the development of an axisymmetric turbulent mixing layer is presented in [6]. Single component LDV measurements of the swirling flow generated by the guide vanes placed at the nozzle exit in the horizontal plane are presented in [7].

Here studied turbulent swirling flow in jet is three-dimensional, inhomogeneous and anisotropic. Generated velocity field is very complex, characterized by inhomogeneity and distinct gradients, especially in the radial direction.

2. EXPERIMENTAL TEST RIG

Swirling flow generator is an axial fan impeller with nine twisted blades with variable angle of attack, designed after the law $rW = \text{const}$. Adjusted angle at the axial fan impeller outlet diameter, which is 0.399 m , is 30° . The dimensionless hub ratio, which represents the ratio of the hub and outer diameter is 0.5 . Inner pipe, i.e. fan casing (Fig. 1, pos. 3), diameter is $D = 0.4\text{ m}$. Experimental test rig, with marked flow direction, is presented in Figure 1, where 1- DC motor is regulated with fully automated thyristor bridge with error up to $\pm 0.5\text{ rpm}$, 2- profiled bell mouth inlet and 3- axial fan impeller with casing.

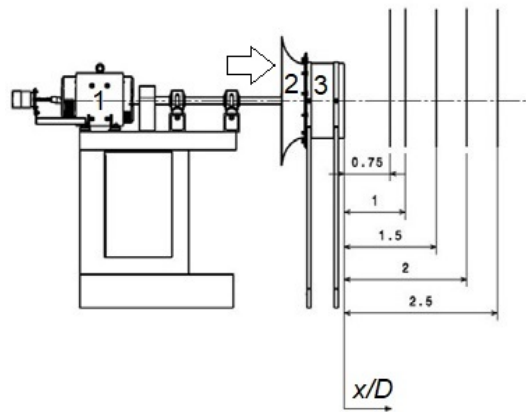


Figure 1. Experimental test rig with marked measuring sections

Three-component LDV measurements have been performed in ten measurement sections along vertical directions at a 10 mm distance each. Measuring sections along the axial fan rotating axis are $x = 300, 400, 600, 800, 1000, 1200, 1400, 1600, 1800$ and 2000 mm , i.e. in the range $x/D = 0.75D$ to $5D$, with the step $0.5D$, except for the first step $0.25D$. In Fig. 1 are presented first five measuring sections.

Measurements have been performed for the axial fan impeller rotation speed $n = 1500\text{ rpm}$. Flow seeding is provided by an Antari Z3000 fog

machine loaded with the Eurolite Smoke Fluid. It was naturally sucked in the test rig by the axial fan.

Three-component LDV system, by TSI, was used in these experiments. Continuum Ar-Ion laser of 5 W , by Coherent is applied. Two probes TSI TR60 with beam expanders XPD60-750 were used to form measurement volume. The TSI Flow Sizer software is used for acquisition and preliminary data analysis. The measurement focus with attached optics was on 757.7 mm . Laser wavelengths were 514.5 nm , 488 nm and 476.5 nm . The measurement volume diameter was app. $70\text{ }\mu\text{m}$, while measurement volume length was app. $280\text{ }\mu\text{m}$. Both LDV probes work in back scatter mode. The velocity was measured with uncertainty lower than 0.1% . [3]. Uncertainty analysis of the used 3D LDV system is thoroughly analyzed and presented in [2, 8].

3. EXPERIMENTAL RESULTS AND DISCUSSIONS

Experimentally obtained distributions of the total velocities along the jet axis are presented in Figure 2. The flow development is observed. Namely, continuous deformation of the velocity profile with gradients in the axial and radial direction occurs. It is obvious that even $5D$ downstream turbulent swirling flow still exists.

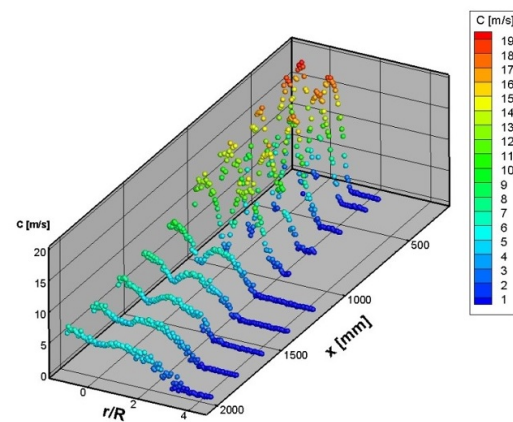


Figure 2. Total velocity distributions $C = C(r, x)$

Circumferential velocity (W) significantly deforms profile of the axial velocity (U). Radial velocity (V) development and distribution is also correlated with the presence and distribution of the circumferential velocity.

Radial-axial distributions of all three velocity components U , V and W in the turbulent swirling jet are presented in the following Figures 3 to 5, where $\varphi = 90^\circ$ denotes upper half of the measuring section, and, consequently, $\varphi = 270^\circ$ lower half. They are obtained on the basis of the Reynolds averaging of the measured instantaneous velocity fields. It is obvious that circumferential velocity significantly

deforms profile of the axial velocity which gains M-shape, with weakly formed reverse, i.e. recirculating flow, in the first two measuring sections, i.e. I and II. The condition for the reverse flow is fulfilled, because swirl number $\Omega > 0.4$ [9]. However, this phenomenon is still not well explained, especially from the mathematical point of view.

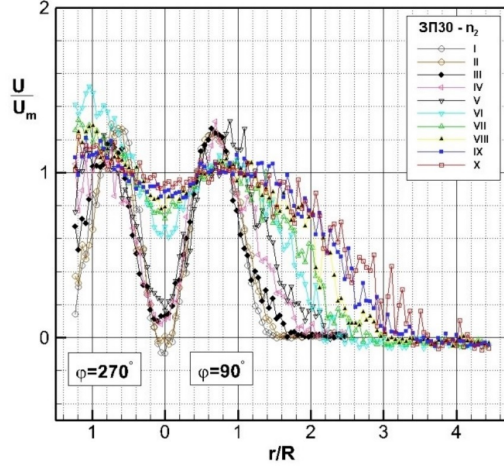


Figure 3. Experimental radial-axial distribution of the axial velocity in the turbulent swirling jet

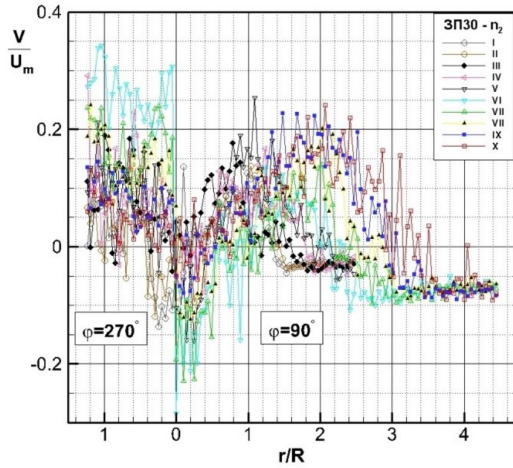


Figure 4. Experimental radial-axial distribution of the radial velocity in the turbulent swirling jet

Swirl number is calculated as follows:

$$\Omega = Q/(RI), \quad (1)$$

while average circulation is determined in the following way:

$$\Gamma = 4\pi^2 R^3 \int_0^1 k^2 U W dk / Q, \quad (2)$$

where $k = r/R$.

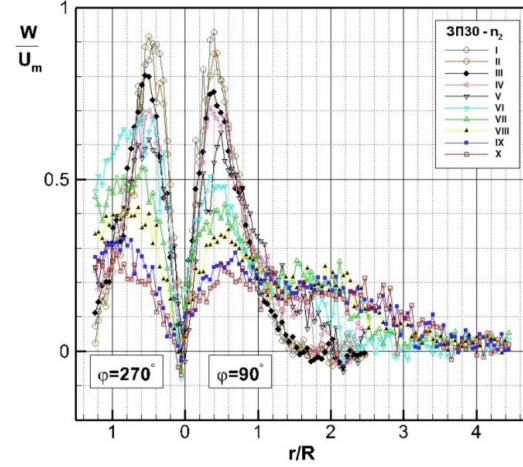


Figure 5. Experimental radial-axial distribution of the circumferential velocity in the turbulent swirling jet

In downstream measuring sections profile of the axial velocity becomes more uniform, with a strict hierarchy of the gradient $\partial_x U > 0$ in a domain $0 < r/R < 0.5$ (Fig. 3). Character of the distribution of the axial velocity, outside this region, points out the expansion of the jet in the radial direction. Maxima values (U_{max}) don't belong to the jet core. That is why the axial velocity profile is concave in the jet axis vicinity, even in the last measuring section X (Fig. 3). Physically, it means that development process is still not finalized, that swirl is still present (Fig. 5) and that the transformation in the axial jet was not possible in the studied case.

Development and transformation of the radial velocity V are also related to the presence and distribution of the circumferential velocity W . Radial velocity profiles in the turbulent swirling jet are very characteristic (Fig. 4). This applies to both the intensity of the radial velocity and its sign. Characteristic domains are the ones where it increases ($\partial_r V > 0$) and decreases ($\partial_r V < 0$), as well as in the points where it changes the sign. It is important for convection and the occurrence of turbulent exchange to analyze the intensity and change in sign of the radial velocity. This is visible in more details in measuring sections: I, III and V (Figs. 6.a-c), where all three velocity components are presented. It is obvious that swirling flow changes character of the radial movement, as well as intensities and signs of the derivative $\partial_r V$. This will be discussed in the case of the measuring section III.

In Figure 6.b are presented distributions of all three velocity components $U_i = U, V$ and W in the measuring section III, where $x = 600$ mm. Average velocity is $U_m = 12.57$ m/s, while Reynolds number is $Re = 358951$ and average circulation, calculated after the Eq. (2), is $\Gamma = 4.93$ m²/s.

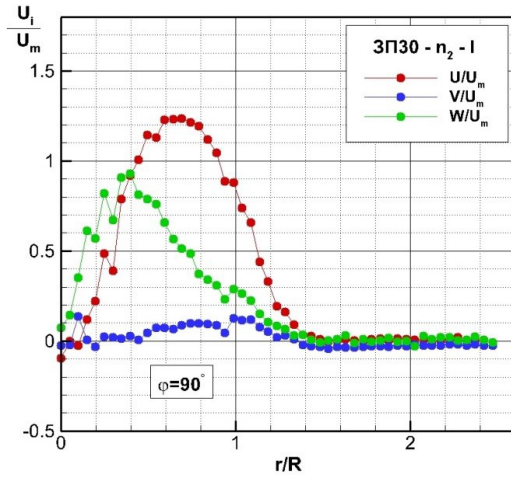


Figure 6.a All three velocities ($U_i = U, V$ and W) distributions in the section I

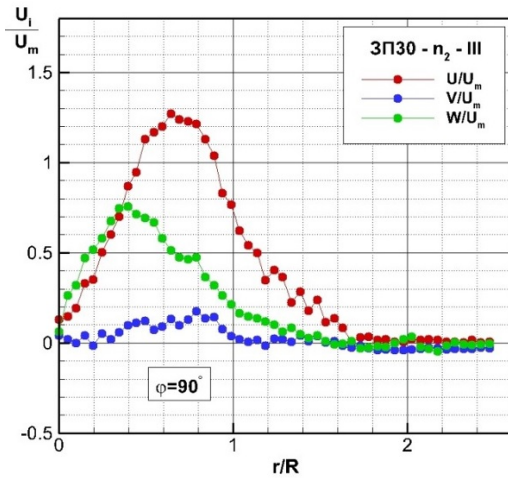


Figure 6.b All three velocities ($U_i = U, V$ and W) distributions in the section III

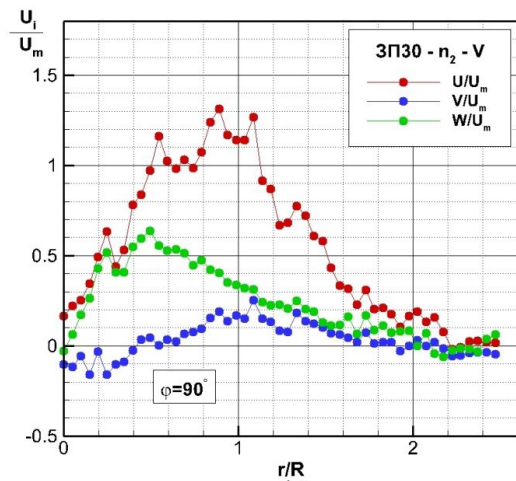


Figure 6.c All three velocities ($U_i = U, V$ and W) distributions in the section V

In the vicinity of the axis gradient of the radial velocity is negative ($\partial_r V < 0$), while in the domain $0.3 < r/R < 0.8$ this gradient is positive ($\partial_r V > 0$). Further increase of the radial coordinate, up to $r/R = 1.2$, results, again, with the negative gradient of the radial velocity ($\partial_r V < 0$). In the region with higher radial coordinate, profile of the radial velocity becomes approximately uniform, so radial gradients $\partial_r V$ have lower values, and the change in its sign, when approaching the jet boundary occurs, with the predominant negative values.

Experiments show that for characteristic points where maxima axial and circumferential velocities are reached, in all measuring sections, stands: $r_{W-max} < r_{U-max}$. With the increase of the axial coordinate x , circumferential velocity W , in region $0 < r/R < 1$, decreases, so that W -profiles, together with its W_{max} are hierarchically distributed from the first (I) up to the last measuring section (X) (Fig. 5). This is not a case outside this region, because profiles intermix and don't follow hierarchy. This leads to more uniform distributions of the circumferential velocity in the downstream measuring sections (Figs. 5 and 6.a-c).

The presented empirical profiles of all three velocities show that in addition to the global maxima (within the respective sections), for example for section III (Fig. 6.b), U_{max} is reached for $r/R \approx 0.65$ and W_{max} for $r/R \approx 0.4$, there is also a significant number of local maxima for all three velocity components.

The complexity of the structure of the averaged velocity field becomes even more obvious when to the previous elements is added the presence of heterogeneous changes of the $\partial_r U_i$ for all three components in the radial direction of the turbulent swirling jet.

Changes of the average velocity fields in radial direction are calculated on the basis of the experimental results presented in Fig. 6.b and presented in Figures 7.a-c. These diagrams have information on the speed of the change of velocity components U_i in radial direction, positions of their maxima, local maxima and minima, as well as correlation of the averaged and fluctuating velocity field. These diagrams could have an important role in analysis of the turbulent swirling jet.

It could be noted in Fig. 7.a that the first zero value ($\partial_r U = 0$) determines value of the maximum velocity $U/U_m(r/R \approx 0.65) = (U/U_m)_{max}$, while diagram on Fig. 7.c provides distribution of the circumferential velocity $W/U_m(r/R \approx 0.4) = (W/U_m)_{max}$.

Changes of the averaged radial velocity in the radial direction are very complex (Fig. 7.b). It is interesting that the intensity of the change of the radial velocity in the measuring section III is significantly higher than the change of the axial velocity, but lower than the circumferential velocity.

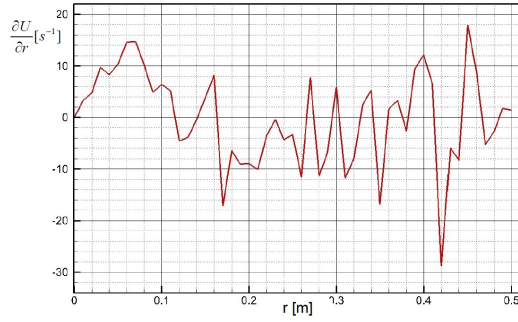


Figure 7.a Change of the average axial velocity in radial direction in the measuring section III

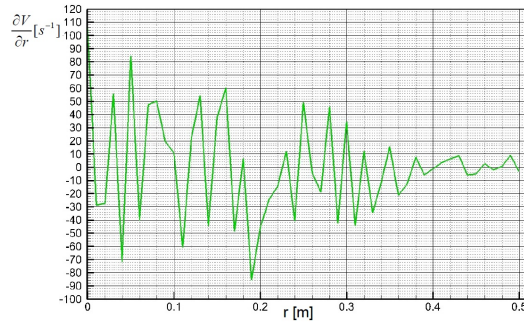


Figure 7.b Change of the average radial velocity in radial direction in the measuring section III

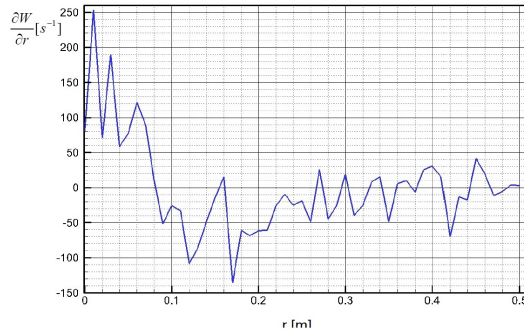


Figure 7.c Change of the average circumferential velocity in radial direction in the measuring section III

This is quantified and presented in the following equation.

$$\begin{aligned} -20 < (\partial_r U)_{\max} < 18, \quad -75 < (\partial_r V)_{\max} < 85, \\ -140 < (\partial_r W)_{\max} < 240. \end{aligned} \quad (3)$$

Value intervals are strongly changeable.

Presented distributions in Figs. 7.a-c are of great importance for Reynolds stresses discussion. It could be theoretically discussed interdependence of the $-\overline{uv}\partial_r V$ which determines production of the important Reynolds shear stress $-\rho\overline{uv}$. In the same

manner mathematical term $-\overline{v^2}\partial_r V$ participates in the generation of the normal turbulent stress $-\rho\overline{v^2}$.

It could be, also, emphasized the important influence of the distribution of the circumferential velocity on the structure of turbulence in the swirling jet. The influence of the mathematical term $-\overline{vw}\partial_r W$ on the production of the Reynolds normal stress $-\rho\overline{w^2}$, as well as the significance of the relation $-\overline{uv}\partial_r W$ on the generation of the turbulent shear stress $-\rho\overline{uw}$ stress could be further discussed.

4. CONCLUSIONS

Conclusions, based on the previously presented experimental results and discussions, could be summarized as follows:

- Measurements have confirmed the assumption of the statistical axisymmetry of the velocity field (Figs. 3-5), what is important from both physical and mathematical point of view.
- Reverse flow occurs in the measuring sections I and II.
- Condition for the reverse flow region is fulfilled, because the swirl number, defined as the $Q/RI\Gamma$, where Q is volume flow rate, R is radius and Γ is circulation is higher than 0.4 when the reverse flow region, after [9] occurs.
- In downstream sections axial velocity becomes more uniform, but in the studied case transformation in the axial jet is not completed.
- Development and transformation of the radial velocity profiles are also correlated with the presence and distribution of the circumferential velocity.
- Intensity and change of the sign of the radial velocity is important for the convection and turbulence exchange.
- Position of the circumferential velocity maximum is correlated to the vortex core diameter, as well as with the vorticity distributions.
- Presented results show that $r_{W\max} < r_{U\max}$ in all measuring sections.
- With increase of the axial coordinate (x) velocity W in the region $0 < r/R < 1$ decreases, so the circumferential velocity profiles are hierarchically distributed downstream from the section I to X. Outside this region this is not a case anymore, and W velocity profiles are mixed.
- The complexity of the structure of the averaged velocity field becomes even more obvious when to the previous elements is

added the presence of heterogeneous changes of the $\partial_r U_i$ for all three components in the radial direction of the turbulent swirling jet.

- It is shown that the changes of the averaged radial velocity in the radial direction are very complex (Fig. 7.b). It is interesting that the intensity of the change of the radial velocity in the measuring section III is significantly higher than the change of the axial velocity, but lower than the intensity of the change of the circumferential velocity.
- All these discussions lead to better understanding of the production of the Reynolds stresses in the generated turbulent swirling jet by the axial fan impeller.

ACKNOWLEDGEMENTS

The results presented in this paper are the result of the research supported by the Ministry of Science, Technological Development and Innovation of the Republic of Serbia under the Agreement on financing the scientific research work of teaching staff at accredited higher education institutions in 2025, no. 451-03-137/2025-03/200105. The work on this paper is finalized during the student demonstrations in Serbia, which started in November 2024. and are still in progress and is dedicated to them who stand for the justice in our society.

REFERENCES

- [1] ISO 5801:2017 “Fans – Performance Testing Using Standardized Airways”. (<https://www.iso.org/standard/56517.html>)
- [2] Janković, N. Z., 2020, “Experimental and Theoretical Research of the Structure of Turbulent Swirl Flow in Axial Fan Jet”, (in Serbian), *Doctoral dissertation, Hydraulic Machinery and Energy Systems Department, Faculty of Mechanical Engineering, University of Belgrade*.
- [3] Janković, N. Z., 2017, “Investigation of the Free Turbulent Swirl Jet behind the Axial Fan”, *Thermal Science*, Vol. 21, Suppl. 3, pp. S771-S782.
- [4] Pratte, B. D., and Keffer, J. F., 1972, “The Swirling Turbulent Jet”, *J. of Basic Eng.*, 94, 4, pp. 739-747.
- [5] Gilchrist, R. T., and Naughton, J. W., 2005, “Experimental Study of Incompressible Jets with Different Initial Swirl Distributions: Mean Results”, *AIAA Journal*, 43, 4, pp. 741-751.
- [6] Mehta, R. D., Wood, D. H., and Clausen, P. D., 1991, “Some Effects of Swirl on Turbulent Mixing Layer Development”, *Physics of Fluids*, 3, 11, pp. 2716-2724.
- [7] Sislian, J. P., and Cusworth, R. A., 1986, “Measurements of Mean Velocity and Turbulent Intensities in a Free Isothermal Swirling Jet”, *AIAA Journal*, 24, 2, pp. 303-309.
- [8] Ilić, J.T., Janković, N.Z., Ristić, S.S., and Čantrak, Đ.S., 2019, “Uncertainty Analysis of 3D LDA System”, Proc., The 7th International Congress of the Serbian Society of Mechanics, Minisymposium M3: Turbulence, Sremski Karlovci, Serbia, Proceedings, paper No. M3j, pp. 189.
- [9] Kitoh, O., 1991, “Experimental Study of Turbulent Swirling Flow in a Straight Pipe”, *J. Fluid Mech.*, Vol. 225, pp. 445-479.